CHIN. PHYS. LETT. Vol. 32, No. 11 (2015) 117401

Superconductivity in Pd-Intercalated Ternary Rare-Earth Polychalcogenide $NdSeTe_2$ *

WANG Pei-Pei(王培培)[1], XUE Mian-Qi(薛面起)[1], LONG Yu-Jia(龙雨佳)[1,2], ZHAO Ling-Xiao(赵凌霄)[1], CAI Yao(蔡瑶)[1], YANG Huai-Xin(杨槐馨)[1], LI Jian-Qi(李建奇)[1,3], REN Zhi-An(任治安)[1,3], CHEN Gen-Fu(陈根富)[1,3]**

[1]*Institute of Physics and Beijing National Laboratory for Condensed Matter Physics, Chinese Academy of Sciences, Beijing 100190*

[2]*Department of Physics, Renmin University of China, Beijing 100872*

[3]*Collaborative Innovation Center of Quantum Matter, Beijing 100190*

(Received 24 July 2015)

We synthesize a set of Pd-doped polycrystalline samples $Pd_xNdSeTe_2$ and measure their physical properties. Compared with pure $NdSeTe_2$, the charge density wave (CDW) order is continuously suppressed with the Pd-intercalation. Bulk superconductivity first appears at $x = 0.06$ with T_c nearly 2.5 K, coexisting with a CDW transition at 176 K. Further Pd-doping enhances T_c, until it reaches the maximum value 2.84 K at x=0.1, meanwhile the CDW transition vanishes. The upper critical field for the optimal doping sample $Pd_{0.1}NdSeTe_2$ is determined from the R–H measurement, which is estimated to be 0.6 T. These results provide another kind of ideal compound for studying the interplay between CDW and superconductivity systematically.

PACS: 74.25.−q, 71.45.Lr, 74.25.F− DOI: 10.1088/0256-307X/32/11/117401

Charge density waves (CDWs) and superconductivity are two distinctive cooperative states that arise from the instabilities of the Fermi surface.[1] The coexistence and competition between CDWs and superconductivity in low-dimensional materials have attracted the interest of a large community for several decades, as they are among the most fundamental problems in condensed matter physics and material science.[2,3] Superconductivity, often emerges in the coexistence of, or in competition with, symmetry-breaking ground states especially antiferromagnetism (AFM) and/or CDW.[4,5] While the rise of iron-based superconductors[6–8] provides many samples that are relevant to AFM and superconductivity, issues on the CDW-superconductivity still require researchers to find more CDW-based superconductors. In recent years, materials including quasi-1D organic conductors,[9] inorganic chain compounds (such as $NbSe_3$),[10] BaBiO system,[11] 1T-$TiSe_2$,[12] $R_{E5}Ir_4Si_{10}$,[13] certain cuprate materials such as $La_{2-x}Sr_xCuO_4$ (LSCO)[14] and $La_{2-x}Ba_xCuO_4$ (LBCO)[15] even $YBa_2Cu_3O_{6.67}$ (YBCO),[16] and more generally, Pd-intercalated binary R_ETe_n (R_E=rare earth; n = 2.5 and 3) compounds[17] and $EuBiS_2F$[18] have presented coexistence and competition between superconductivity and CDW order. Here we further expand this kind of material to ternary rare-earth polychalcogenide system for better understanding the relationship between CDW and superconductivity.

$NdSeTe_2$ has been chosen as the representative of ternary rare-earth polychalcogenide $LnSeTe_2$ (Ln=La, Ce, Pr, Nd and Sm), a series of typical CDW materials. $NdSeTe_2$ possesses the same structure as rare-earth tritellurides R_ETe_3 (R_E=Y, La–Lu),[19,20] which is crystallized with the $NdTe_3$ type in space group $Cmcm$ (No.63).[21] Figure 1(a) shows the crystal structure of $NdSeTe_2$, exhibiting highly two-dimensional characteristic. Double sheets of nearly square planar tellurium Te are separated by a corrugated NdSe slab, the NdSe-slab and Te-sheet are stacked along the b-axis. The double square Te layers play an important role in the physical properties of $NdSeTe_2$, due to the fact that they usually prefer distortions and generation of commensurate or incommensurate CDWs rather than the high-symmetry square arrangement.[22] In this study, we present the continuous suppression of the CDW order in $NdSeTe_2$ with the appearing of the superconductivity through Pd intercalation.

Polycrystalline samples of $Pd_xNdSeTe_2$ ($0 \leq x \leq 0.5$) were synthesized by the solid-state reaction method. Stoichiometric amounts of rare earth elements Nd(3N5), Te(5N), Se(5N), and Pd(3N) powders were weighed and mixed in a glove box with protective argon atmosphere, then the mixed materials were sealed in a thick walled quartz tube under vacuum. The quartz tube was heated to 650℃ in 6 h and held for 50 h. After cooling to room temperature naturally, the resulting product was reground, pressed into a pel-

*Supported by the National Basic Research Program of China under Grant No 2015CB921303, and the Strategic Priority Research Program (B) of the Chinese Academy of Sciences under Grant No XDB07020100.

**Corresponding author. Email: gfchen@iphy.ac.cn

© 2015 Chinese Physical Society and IOP Publishing Ltd

let, sealed in an evacuated quartz tube and reheated for another 50 h at 650℃. Then the homogeneous samples were obtained.

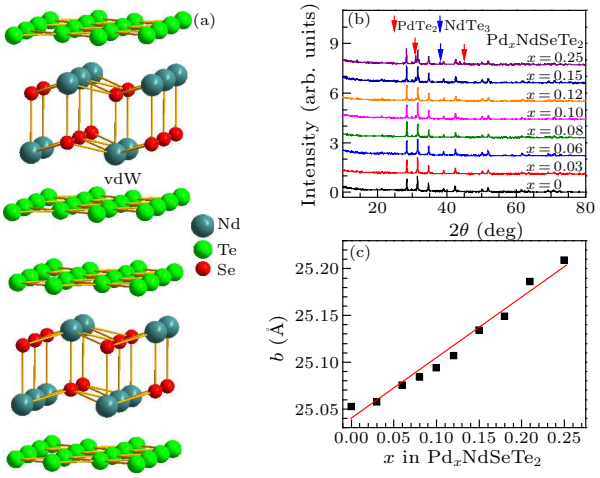


Fig. 1. (a) The crystal structure of $NdSeTe_2$, vdW is the Van der Waals gap between the double Te layers. (b) Powder XRD data of $Pd_xNdSeTe_2$ with different nominal Pd contents. Impurity phases, as marked by the red and blue arrows, appear only for the samples with high doping level. (c) Lattice parameter b as a function of x in $Pd_xNdSeTe_2$.

The x-ray diffraction (XRD) pattern of the resulting samples was taken on a PANalytical diffractometer by using Cu $K\alpha$ radiation at room temperature. Magnetization measurements were carried out in MPMS SQUID VSM (Quantum Design) with zero-field-cooled (ZFC) and/or field-cooled (FC) modes. Transport properties were measured in a PPMS system (Quantum Design). The microstructure analysis and in situ transmission electron microscopy (TEM) observations were performed on a Tecnai F20 transmission electron microscope, equipped with low-temperature holders.

As shown in Fig. 1(a), Pd ions are considered to be intercalated into the vdW gap between double Te sheets, which will give rise to expansion of the unit cell. Figure 1(b) shows the powder x-ray diffraction patterns of nominal Pd content samples $Pd_xNdSeTe_2$ ($0 \leq x \leq 0.25$), which can be well indexed by using the orthorhombic crystal structure ($NdTe_3$-type). Impurity phases ($PdTe_2$ and $NdTe_3$) appear only for samples with high doping level ($x > 0.12$). To exclude the effect of impurity phase, we have synthesized a pure $PdTe_2$ sample, no superconducting transition was observed in both transport and magnetic susceptibility measurements as temperature went down to 1.8 K. Further detailed analysis of the x-ray data gives the lattice constant b, as shown in Fig. 1(c), which clearly shows that the lattice constant b increases with the Pd content x, indicating the successful intercalation of Pd into the weakly bonded double Te layers. It should be noted that, as the formation of impurity phases mostly is $PdTe_2$, the actual Pd content deviates from the nominal content at high doping level. Using energy dispersive x-ray spectroscopy (EDX), the actual Pd contents in this serial samples have been determined.

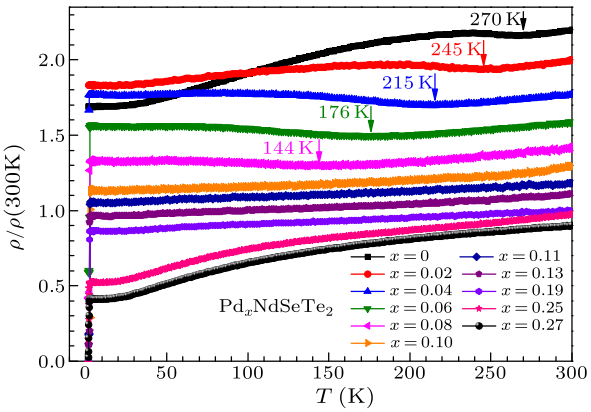


Fig. 2. Normalized temperature-dependent resistivity data measured on Pd-intercalated samples $Pd_xNdSeTe_2$. CDW transition moves to lower temperature as Pd content increases. All curves are moved with a certain distance for better clarity.

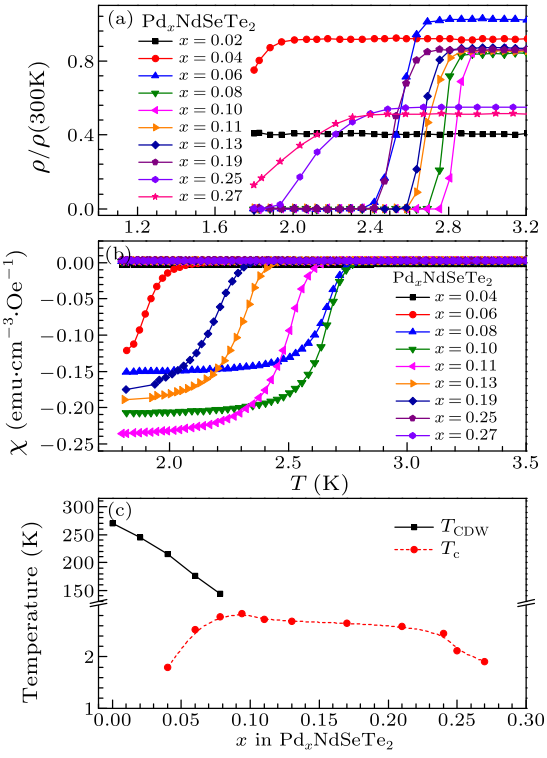


Fig. 3. Superconducting properties of actual Pd content samples $Pd_xNdSeTe_2$. (a) T-dependent resistivity in an expanded region at low temperature. (b) Superconducting phase transition confirmed by dc magnetic susceptibility $\chi(T)$. (c) Electronic phase diagram for $Pd_xNdSeTe_2$. Squares and circles correspond to the CDW and superconducting transition temperature, respectively.

The resistivity of pure $NdSeTe_2$ sample is shown in Fig. 2. It has an anomaly associated with the CDW transition at approximately 270 K, which is lower than the single crystal based measurement,[23] and a good

metallic behavior below 250 K. Generally, the formation of CDW removes electrons and opens a gap at the Fermi surface (FS), which would lead to a semiconducting or insulating state. However, the metallic behavior below $T_{\rm CDW}$ can be explained by the partial nesting effect of FS.[24,25] While some parallel planar sections of the FS nests, other parts of the FS remain unaffected and are responsible for conductivity and superconductivity. With Pd intercalation, the CDW changed and evolved interestingly. We can see that, with increasing amounts of Pd, the anomaly becomes broader and moves to the lower temperature. The zero resistance emerges at $x = 0.06$, while a less pronounced anomaly is still observed at around 176 K. At $x = 0.1$, the anomaly disappeared resistivity shows a metallic behavior, meanwhile $T_{\rm c}$ reaches the maximum value 2.84 K. Further Pd doping does not change the metallic behavior, which is similar to the Cu doping $1T$-$TiSe_2$, and $T_{\rm c}$ is found to drop slightly when $x > 0.1$. For better clarity, the expanded plots of the resistivity around $T_{\rm c}$ are shown in Fig. 3(a). For $x = 0.04$, the resistivity drops obviously at 1.8 K, which implies the phase transition from normal state to superconducting state. For other different Pd content samples we can determine $T_{\rm c}$ to be 2.53 K(0.06), 2.78 K(0.08), 2.84 K(0.10), 2.67 K(0.11), 2.69 K(0.13) and 2.52 K(0.19).

Superconductivity in $Pd_xNdSeTe_2$ was also confirmed by dc magnetic susceptibility with zero-field-cooled (ZFC) and field-cooled (FC) under 10 Oe. Below $x = 0.06$, no superconductivity transition could be observed down to the lowest temperature of our measurement 1.8 K. At $x = 0.06$, an obvious drop in the magnetic susceptibility just begins to appear as the temperature is lowered to 2.53 K (Fig. 3(b)), suggesting the onset of a superconducting transition. With increasing the Pd content, both superconducting transition temperature and diamagnetic signal increase and reach the maximum at $x = 0.1$, for which the shielding volume fraction is estimated to be over 100%, which imply the bulk superconductivity in the sample. The shielding response of larger than 100% is due to the effect of demagnetization. Further increasing x results in suppression of signal strength or transition temperature. The evolution of $T_{\rm c}$ with increasing the Pd content observed from susceptibility measurement is also consistent with the resistivity data. Figure 3(c) is the phase diagram showing $T_{\rm CDW}$ and $T_{\rm c}$ as a function of actual Pd content in $Pd_xNdSeTe_2$. The phase diagram is quite similar to that of Cu_xTiSe_2,[12] where the superconductivity emerges when the CDW order is suppressed by doping. However, one should note that an important difference between the two is that, for Cu-intercalated $1T$-$TiSe_2$, the doped electrons enter the bottom of the Ti $3d$-induced conduction band, which dominates the electronic properties,[26,27] while the Pd atom has a $4d^{10}5s^0$ configuration, it seems that no electron transfer takes place between Pd and $NdSeTe_2$.[28] Taking consideration of the structural similarity to R_ETe_n, we suppose that the Fermi surface of $NdSeTe_2$ is also derived mainly by the p-orbits of the Te atoms, which are formed by the double layers of nearly square-planar sheets, and the contribution near $E_{\rm F}$ from R_E $4f$ states may be negligible.[29,30] Further theoretical and spectroscopic studies will be helpful to understand the underlying mechanism.

Another important parameter of superconductors is the upper critical field H_{c_2}. Figure 4(a) shows the temperature-dependent resistivity of the optimal doping sample $Pd_{0.1}NdSeTe_2$ under different magnetic fields. With increasing the magnetic field, the transition temperature $T_{\rm c}$ shifts to lower temperature and the transition width gradually becomes broader, suggesting the strong anisotropy of the critical field,[31] as expected from the two-dimensional electronic structure. At $H = 0.6$ T, the superconducting transition almost cannot be observed above 1.8 K. The corresponding upper critical field H_{c_2} versus $T_{\rm c}$ is plotted in Fig. 4(b), where $T_{\rm c}$ is defined by a criterion of 90% of normal state resistivity. Since the Pauli limiting field $H_{\rm p} = 1.84T_{\rm c} > 0.6$ T, the mainly pair-breaking mechanism in the $Pd_{0.1}NdSeTe_2$ is the orbital effect. According to the conventional one-band Werthamer–Helfand–Hohenberg formula $H_{c_2}(0) = -0.69(dH_{c_2}/dT)T_{\rm c}$, which describes the orbital limited upper critical field of type-Ⅱ superconductors, the value of $dH_{\rm c}/dT$ is -0.31 for $Pd_{0.1}NdSeTe_2$, and taking $T_{\rm c} = 2.84$ K, the upper critical field is estimated to be 0.61 T.

In the previous work, we have reported the superconductivity in $Pd_xR_ETe_3$,[17] in which we found that, for heavy rare earth elements with smaller ionic radius, Y and Gd–Tm, the CDW transition temperatures $T_{\rm CDW}$ are relatively low (240–380 K) and the superconducting transition temperatures $T_{\rm c}$ are relatively high (2–3 K); while for light rare earth elements with larger ionic radius, La–Nd, $T_{\rm CDW}$ are higher (greater than 450 K) and $T_{\rm c}$ are lower (less than 0.6 K). No superconductivity was observed in Pd_xCeTe_3 and Pd_xNdTe_3 as temperature down to 50 mK. The absence of superconductivity in Pd_xCeTe_3 may be ascribed to the hybridization of the $4f^1$ electrons with itinerant conduction electrons, while it may not be the same for Pd_xNdTe_3 as Nd^{3+} ions are well localized.[17] However, in $NdSeTe_2$, a compound which can be thought of as substitution of Se atoms for Te in the RTe slab in $NdTe_3$, the CDW transition temperature decreases from higher than 450 K in $NdTe_3$ to less than 300 K in $NdSeTe_2$. On this basis, Pd-intercalation in the double Te layer further suppresses the CDW transition and leads to superconductivity with the highest $T_{\rm c}$ of 2.84 K.

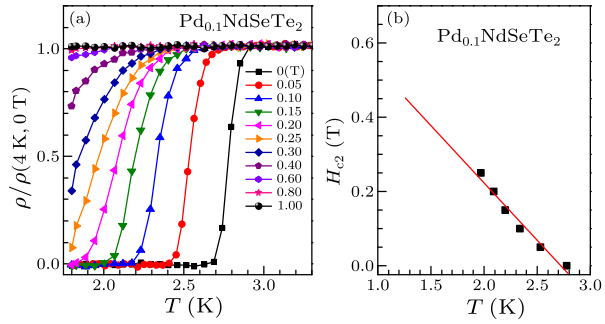


Fig. 4. (a) Characterization of the superconductivity in $Pd_{0.1}NdSeTe_2$ under magnetic field. (b) The $H_{c_2}(T)$ diagram determined from $\rho(H)$ data.

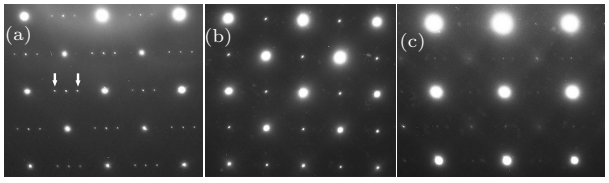


Fig. 5. (a) The $T = 100$ K electron diffraction patterns of the $NdSeTe_2$. (b) The $T = 300$ K electron diffraction patterns of the $NdSeTe_2$. (c) The $T = 100$ K electron diffraction patterns of the superconducting sample $Pd_{0.1}NdSeTe_2$.

To directly probe the structural features relevant to the CDW transition in this ternary rare-earth polychalcogenide system, electron diffraction experiments were performed on pure $NdSeTe_2$ and optimal superconducting sample $Pd_{0.1}NdSeTe_2$, as shown in Fig. 5. Our measurements at 100 K (Fig. 5(a)) clearly show that there exist super-reflections due to the structure modulations accompanied by the formation of charge density waves, compared with the normal state results in Fig. 5(b) at 300 K. While for the superconducting samples of $Pd_{0.1}NdSeTe_2$ at 100 K shown in Fig. 5(c), the intensity of the superstructure spots evidently decreased, indicating the suppression of CDW by the Pd intercalation. When shown in combination with temperature-dependent resistivity data and magnetic susceptibility data, these facts clearly demonstrate the competition between CDW and superconductivity in $Pd_xNdSeTe_2$.

In conclusion, we have successfully adjusted a ternary rare-earth polychalcogenide CDW material-$NdSeTe_2$ to be a superconductor via palladium intercalation. A superconducting signal first appears in $Pd_xNdSeTe_2$ at Pd content of 4%, bulk superconductivity emerges at Pd content of 6% with T_c nearly 2.5 K and reaches a maximum of 2.84 K at 10%. Further Pd-doping suppresses T_c to a lower temperature. Our finding offers an ideal compound for systematic study of the interplay between CDWs and superconductivity. Furthermore, the successful adjusting of superconductivity in $Pd_xNdSeTe_2$ can also provide a guideline to exploring superconductivity in other ternary rare-earth polychalcogenide materials.

References

[1] Grüner G 1988 *Rev. Mod. Phys.* **60** 1129
[2] Wu T et al 2013 *Nat. Commun.* **4** 2113
[3] Barišić N et al 2013 *Nat. Phys.* **9** 761
[4] Joe Y I et al 2014 *Nat. Phys.* **10** 421
[5] Zhang S C 1997 *Science* **275** 1089
[6] Kamihara Y et al 2008 *J. Am. Chem. Soc.* **130** 3296
[7] Chen G F et al 2008 *Phys. Rev. Lett.* **100** 247002
[8] Ren Z A et al 2008 *Chin. Phys. Lett.* **25** 2215
[9] Jérome D 2004 *Chem. Rev.* **104** 5565
[10] Nunezregueiro M et al 1993 *Synth. Met.* **56** 2653
[11] Mattheiss L F et al 1988 *Phys. Rev.* B **37** 3745
[12] Morosan E et al 2006 *Nat. Phys.* **2** 544
[13] Singh Y et al 2005 *Phys. Rev.* B **72** 45106
[14] Torchinsky D H et al 2013 *Nat. Mater.* **12** 387
[15] Fujita M et al 2004 *Phys. Rev.* B **70** 104517
[16] Chang J et al 2012 *Nat. Phys.* **8** 871
[17] He J B et al 2013 arXiv:1301.3032[cond-mat.supr-con]
[18] Zhai H F et al 2014 *Phys. Rev.* B **90** 064518
[19] Lin W et al 1965 *Inorg. Chem.* **4** 877
[20] Norling B K et al 1966 *Inorg. Chem.* **5** 1488
[21] Fokwa Tsinde B P et al 2005 *Solid State Sci.* **7** 573
[22] Patschke R et al 2002 *Phys. Chem. Chem. Phys.* **4** 3266
[23] Wang P P et al 2015 *Chin. Phys. Lett.* **32** 087101
[24] Yokoya T et al 2005 *Phys. Rev.* B **71** 140504
[25] Felser C et al 1998 *J. Mater. Chem.* **8** 1787
[26] Qian D et al 2007 *Phys. Rev. Lett.* **98** 117007
[27] Jeong T et al 2007 *Phys. Rev.* B **76** 153103
[28] Morosan E et al 2010 *Phys. Rev.* B **81** 094524
[29] Brouet V et al 2004 *Phys. Rev. Lett.* **93** 126405
[30] Laverock J et al 2005 *Phys. Rev.* B **71** 085114
[31] Campbell A M and Evetts J E 1972 *Adv. Phys.* **21** 199